

Physical gels made of liquid crystalline B₄ phase†Cite this: DOI: 10.1039/c3cc41225c Anna Zep,^a Mirosław Salamonczyk,^a Nataša Vaupotič,^{b,c} Damian Pocięcha^a and Ewa Gorecka^{*a}Received 15th February 2013,
Accepted 27th February 2013

DOI: 10.1039/c3cc41225c

www.rsc.org/chemcomm

The achiral liquid crystalline materials showing two B₄ (HN) phases have been found to exhibit strong gelation ability for various organic solvents with reversible sol–gel phase transition. The gel is formed by helical tubules, which build entangled 3D network, encapsulating the solvent. The equilibrium of left- and right-handed tubules is preserved in the gel, even if the chiral solvent is used.

The chemical and physical organogels are formed by the self-assembly of organic molecules into a 3D fiber network that entraps different types of organic solvents. The fibers of chemical gels are built of covalently bonded polymers. In the case of the physical gels the fibrous aggregates are formed by low mass molecules connected through the non-covalent interactions such as hydrogen bonding,^{1–5} π–π,⁶ lipophilic,⁷ dipole–dipole interactions,⁸ donor–acceptor exchange,⁹ etc. In recent years growing interest in gelators with liquid crystalline properties has been observed. There are several examples of mesogenic materials that exhibit gelation abilities in organic solvents. Mamiya *et al.* reported that chiral azobenzene derivatives, which exhibit smectic phases, are capable of forming fibrous aggregates with smectic order.⁸ Hashimoto *et al.*,¹⁰ Isoda *et al.*¹¹ and Yoshio *et al.*¹² described the liquid-crystalline disc-like compounds that form physical gels in organic solvents with fibers exhibiting columnar structure. Here we report a new type of mesogenic gelators, which give the B₄ phase in the bulk sample. The B₄ phase is one of the most unusual liquid crystalline (LC) phases; it draws a lot of attention because of its chiral nature and strong optical activity, despite the fact that it is built of achiral molecules.¹³ The structure of the phase was attributed to the local saddle-splay curvature of membranes, made of a few molecular layers. Such elastic deformation leads to helical nanofilaments (HN), *i.e.* twisted ribbons, with single filament

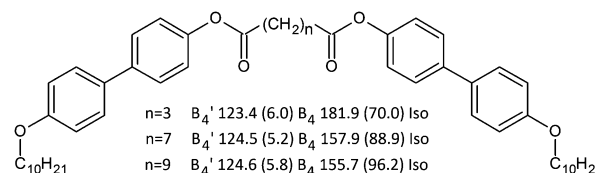


Fig. 1 General molecular structure of the studied dimers; phase transition temperatures (°C) and enthalpy changes (J g⁻¹) are also given.

having a well-defined diameter.¹⁴ Recently it has been shown that the filament morphology is preserved even if the B₄ material is mixed with mesogens forming nematic, smectic or columnar phases.^{15–17}

Formation of the gel seems to be a general feature of the B₄ materials, independently of their molecular architecture. Here we describe the gelation ability of symmetric mesogenic dimers (Fig. 1) made of 4-decyloxy-4'-hydroxybiphenyl units connected by flexible alkyl spacers with an odd number of carbon atoms (synthesis described in ESI†).¹⁸ These materials are thermotropic liquid crystals, exhibiting two B₄-type phases.

The LC properties for all the studied homologues are presented in Fig. 1. The formation of the B₄-type phases was confirmed by characteristic optical textures, with low birefringence and large optically active domains observed when the sample is cooled from the isotropic phase. The optical texture was not affected by the B₄–B₄' phase transition. There were no noticeable changes either in the optical activity or in the domain shape or size. In both phases the X-ray diffraction measurements revealed a robust lamellar structure evidenced by up to 7 harmonics of the main signal, related to the layer thickness (Fig. 2). Significant broadening of these signals indicates a finite size of a lamellar membrane, from which filaments of the B₄ phase are formed (line broadening due to a small size of crystallites¹⁹); the correlation length along the layer normal, determined from diffraction signals width, is only 3–4 layers. The reflections observed at high angles confirm that molecules exhibit long range order within layers (Fig. 2).

Signals in the diffraction pattern for compound *n* = 9 in the B₄ phase can be fitted to the monoclinic crystallographic lattice with parameters *a* = 9.30 Å, *b* = 5.35 Å, *c* = 56.7 Å and *γ* = 110°.

^a Department of Chemistry, University of Warsaw, Żwirki i Wigury 101, 02-089 Warsaw, Poland. E-mail: gorecka@chem.uw.edu.pl

^b Department of Physics, Faculty of Natural Sciences and Mathematics, University of Maribor, Koroška 160, 2000 Maribor, Slovenia

^c Jožef Stefan Institute, Jamova 39, 1000 Ljubljana, Slovenia

† Electronic supplementary information (ESI) available: Experimental details, synthesis of materials and their spectral characterization. See DOI: 10.1039/c3cc41225c

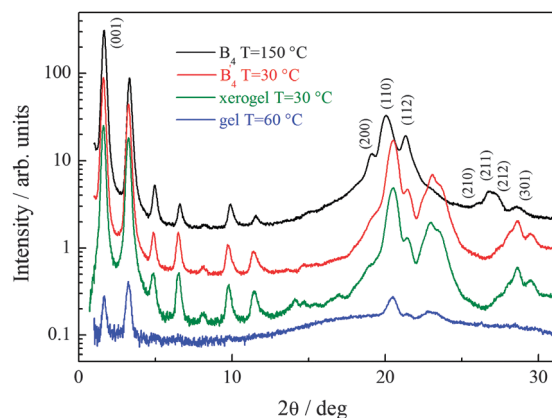


Fig. 2 X-ray pattern of the B_4 and B_4' phase, xerogel and gel of compound with $n = 9$ with toluene.

Since $a/b = 1.73$, one can deduce that molecular mass centres form nearly ideal hexagons in the smectic planes; the molecules are tilted to the next nearest neighbour. The observed hkl signals with $l = 1$ and 2 indicate the presence of some interlayer correlations. The structure of the B_4' phase is similar to the B_4 phase; the same layer thickness is observed. The changes in the high angle signals show that the phases differ in their in-plane order of molecules.

All the studied compounds were excellent gelators for various organic fluids: toluene, nitrobenzene, 3-methylcyclohexanone, (–)-menthone, (+)-menthone, chloroform and dichloromethane, already at concentrations *ca.* 5 wt%. No gelation was observed for polar organic solvents (DMF, ethanol, methanol). The gels were formed when the mixture of LC and solvent is heated and subsequently cooled to room temperature; it should be stressed that gelation occurred in the whole volume of the sample, no precipitation of crystallites from solution was observed (Fig. 3). The gel and sol states are thermo-reversible with the phase transition temperature dependent on the organic solvent (Table 1). The sol–gel phase transition temperatures monitored optically coincide with those detected by the DSC method (Fig. 4) and are much lower than the B_4 -Iso phase transition in pure materials.

The morphology of gels was examined by the scanning electron microscopy (SEM). The SEM picture (Fig. 3) revealed formation of a three-dimensional network composed of long, entangled fibres; the filaments are made of tightly wound,

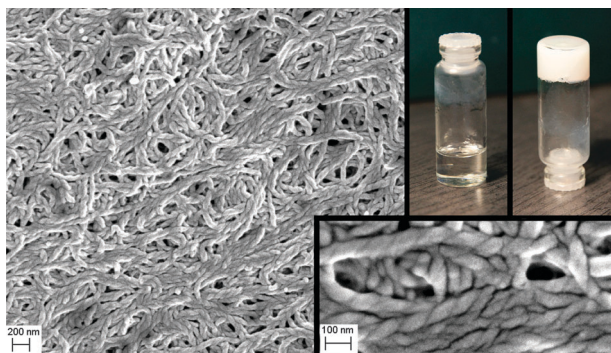


Fig. 3 SEM image of xero-gel formed from compound $n = 7$ in (–) menthone, after evaporation of solvent; enlarged picture shows helical tubular filaments. Photos of material in vial indicate that sol and gel states have similar volumes.

Table 1 Sol–gel phase transition temperatures for dimer $n = 9$ (~5%) in different organic solvents. In the table only phase transition temperatures are given (taken as peak position in heating runs), as the enthalpies ($\sim 80 \text{ J g}^{-1}$) are measured with large error due to some evaporation of the solvent at elevated temperatures, despite the sealing of the samples

Solvent	Sol–gel phase transition temperature ($^{\circ}\text{C}$)
Toluene	75.0
Nitrobenzene	85.0
(<i>R</i>)-(+)-3-Methylcyclohexanone	81.0
(+)-Menthone	86.0
(–)-Menthone	86.0

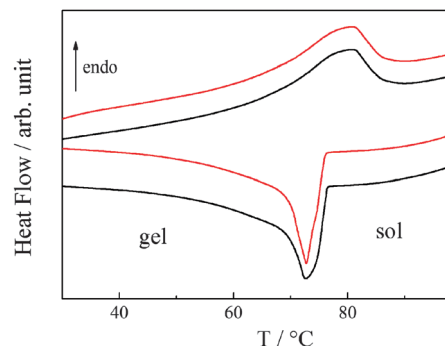


Fig. 4 DSC scans (two consecutive runs, $\pm 10 \text{ deg min}^{-1}$) showing reversible sol–gel transition for dimer $n = 9$ in (*R*)-(+)-3-methylcyclohexanone.

helical tubules. The gel is formed by encapsulating the solvent within the network of percolated gelator and inside the tubes. Both right- and left-handed helical tubules are present; the equilibrium between the helices of opposite sense is not broken even if an optically pure solvent (menthone) is used. The average diameter, d , of the nanofilament is 50 nm, and the helical pitch, L , ~ 40 –50 nm, which gives the aspect ratio $d/L \sim 1$; the values were not dependent on the homologue used for gel preparation.

The X-ray pattern of the gel (as well as dried xero-gel) (Fig. 2) is similar to the X-ray pattern of the B_4' phase. It shows signals coming from the lamellar structure and a few reflections at high angles. The X-ray signals from the crystal structure disappear at the gel–sol phase transition, so above T_c only a diffused signal from the solvent is observed. On subsequent cooling below the sol–gel phase transition temperature the X-ray pattern of the B_4' phase is recovered. Therefore, we can conclude that the fibres forming gels have the structure of the bulk B_4' phase. This also shows that the material which forms tubules is not diluted by the solvent.

The morphology of the gel was compared with that observed for the bulk material. The AFM picture of the B_4' phase (Fig. 5) shows strongly distorted twisted ribbons, made of membranes 5–6 layers thick, with the orientation of the layer normal perpendicular to the local twist axis. The layer thickness estimated from the AFM picture is consistent with the spacing measured by the X-ray method. The AFM picture seems to confirm the saddle-splay helical structure of the B_4 phase, proposed by the Boulder group.¹⁴

The formation of the gel was also checked for a few other bent core materials (see ESI†). Gel was formed for the compounds

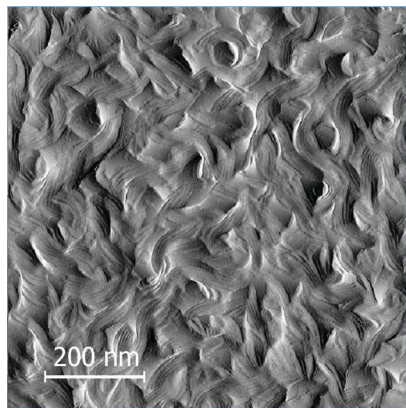


Fig. 5 AFM picture of the B_4' phase of compound with $n = 9$ at room temperature.

exhibiting the B_4 (HN) phase, while it was not observed for materials showing the dark conglomerate (DC) phase. The DC phase exhibits non-birefringent but optically active texture similar to the B_4 phase; however its X-ray pattern is typical for smectics with liquid like order inside the smectic layers; for this phase a sponge like structure with saddle-splay curvature was assumed.²⁰ Thus it seems that for this class of compounds the crystalline character of the layers is an important factor for the formation of filaments with gelation ability.

In summary, there are two basic types of a helical filament structures that can accommodate the local twist of smectic layers: twisted ribbons and helical tubules.²¹ The theoretical model, proposed for amphiphilic systems, predicts that the helical tubular vs. twisted ribbon morphology should be biased by the in-plane crystallinity of the membrane, from which filaments are made.²² This is apparently not the case for the system studied here, as both types of filaments, tubules and ribbons are formed from smectic with crystal-like in-plane order. In the studied system twisted ribbons are formed in bulk (B_4 phase) while in solvent helical tubules are favored. This shows that the surrounding is of primary importance for the morphology of the objects. The result can be justified if one notices that the formation of tubules in bulk material would require molecules in the center of the tube being in a molten state (in the nematic or isotropic phase); that would cost the system some additional energy; while in the liquid solvent the inner part of a tube can be filled with the molecules of the solvent. Additionally, tubes are stabilized in solutions, since the membrane edge exposed to the solvent is much smaller for tubes than for twisted ribbons. This mechanism should be especially effective in systems in which the edges are polar. In isotropic fluid tubular filaments easily percolate trapping the solvent, forming the gel state.

It was suggested that the helix sense of ribbons is related to the symmetry breaking at the molecular level – formation of chiral conformers of achiral bent-core molecules.¹⁴ However, helices of both handedness are observed in the chiral solvent, although in such an environment stabilization of one of the chiral conformers

would be expected. Alternatively, left- or right-handed tubules can be obtained from the membranes when they try to accommodate the spontaneous splay of polarization, which is an inherent property of the bent-core liquid crystals and is promoted by the surfaces (thus by a finite width of the ribbon). A similar effect, *i.e.* the variation in the tilt direction in smectic C phase was shown to promote the formation of cylindrical tubules and helical ribbons of chiral lipid membranes.^{21,23}

The authors wish to thank Prof. M. Čepič for all the discussions and acknowledge the FNP Project TEAM/2010-5/4, Self-assembly of functionalized inorganic–organic liquid crystalline hybrids for multifunctional nanomaterials, for financial support. Special thanks to Dr E. Bialecka-Florjanczyk for drawing our attention to this class of dimeric mesogens.

Notes and references

- 1 K. Hanabusa, M. Yamada, M. Kimura and H. Shirai, *Angew. Chem., Int. Ed. Engl.*, 1996, **35**, 1949.
- 2 J. van Esch, F. Schoonbeek, M. de Loos, H. Kooijman, A. L. Spek, R. M. Kellogg and B. L. Feringa, *Chem.–Eur. J.*, 1999, **5**, 937.
- 3 K. Yoza, N. Amanokura, Y. Ono, T. Akao, H. Shinmori, M. Takeuchi, S. Shinkai and D. N. Reinhoudt, *Chem.–Eur. J.*, 1999, **5**, 2722.
- 4 A. Aggeli, M. Bell, N. Boden, J. N. Keen, P. F. Knowles, T. C. B. McLeish, M. Pitkeathly and S. E. Radford, *Nature*, 1997, **386**, 259.
- 5 R. J. H. Hafkamp, M. C. Feiters and R. J. M. Nolte, *J. Org. Chem.*, 1999, **64**, 412.
- 6 F. Placin, M. Colomes and J.-P. Desvergne, *Tetrahedron Lett.*, 1997, **38**, 2665.
- 7 K. Murata, M. Aoki, T. Suzuki, T. Harada, H. Kawabata, T. Komori, F. Ohseto, K. Ueda and S. Shinkai, *J. Am. Chem. Soc.*, 1994, **116**, 6664.
- 8 J. Mamiya, K. Kanie, T. Hiyama, T. Ikeda and T. Kato, *Chem. Commun.*, 2002, 1870.
- 9 D. Rizkov, J. Gun, O. Lev, R. Sicsic and A. Melman, *Langmuir*, 2005, **21**, 12130.
- 10 M. Hashimoto, S. Ujiie and A. Mori, *Adv. Mater.*, 2003, **15**, 797.
- 11 K. Isoda, T. Yasuda and T. Kato, *J. Mater. Chem.*, 2008, **18**, 4522.
- 12 M. Yoshio, R. Konishi, T. Sakamoto and T. Kato, *New J. Chem.*, 2013, **37**, 143.
- 13 T. Sekine, T. Niori, J. Watanabe, T. Furukawa, S. W. Choi and H. Takezoe, *J. Mater. Chem.*, 1997, **7**, 1307.
- 14 L. E. Hough, H. T. Jung, D. Kruerke, M. S. Heberling, M. Nakata, C. D. Jones, D. Chen, D. R. Link, J. Zasadzinski, G. Heppke, J. P. Rabe, W. Stocker, E. Korblova, D. M. Walba, M. A. Glaser and N. A. Clark, *Science*, 2009, **325**, 456.
- 15 T. Otani, F. Araoka, K. Ishikawa and H. Takezoe, *J. Am. Chem. Soc.*, 2009, **131**, 12368.
- 16 D. Chen, M. S. Heberling, M. Nakata, L. E. Hough, J. E. MacLennan, M. A. Glaser, E. Korblova, D. M. Walba and N. A. Clark, *ChemPhysChem*, 2012, **13**, 155.
- 17 D. Chen, C. Zhu, H. Wang, J. E. MacLennan, M. A. Glaser, E. Korblova, D. M. Walba, J. A. Rego, E. A. Soto-Bustamante and N. A. Clark, *Soft Matter*, 2013, **9**, 462.
- 18 E. Bialecka-Florjanczyk, I. Sledzinska, E. Gorecka and J. Przedmojski, *Liq. Cryst.*, 2008, **35**, 401.
- 19 P. Scherrer, *Goettingen Nachr. Ges.*, 1918, **2**, 98.
- 20 D. Chen, M. S. Heberling, M. Nakata, L. E. Hough, J. E. MacLennan, M. A. Glaser, E. Korblova, D. M. Walba and N. A. Clark, *ChemPhysChem*, 2012, **13**, 155.
- 21 J. V. Selinger, M. S. Spector and J. M. Schnur, *J. Phys. Chem. B*, 2001, **105**, 7157.
- 22 R. Oda, I. Huc, M. Schmutz, S. J. Candau and F. C. MacKintosh, *Nature*, 1999, **399**, 566.
- 23 J. V. Selinger, F. C. MacKintosh and J. M. Schnur, *Phys. Rev. E*, 1996, **53**, 3804.